Proc. Indian Acad. Sci. (Earth Planet. Sci.), Vol. 90, Number 1, March 1981, pp. 1–26.

Windows to early solar system processes : Refractory inclusions in the CV and CM chondrites*

J D MACDOUGALL and J N GOSWAMI**
Scripps Institution of Oceanography, La Jolla, California 92093, USA
** Physical Research Laboratory, Ahmedabad 380 009, India

MS received 7 February 1981

Abstract. The refractory element-enriched inclusions found in the carbonaceous meteorites give cosmochemists a fascinating glimpse at processes which occurred near the birth of the solar system. Although many complications must still be unravelled, the weight of the available evidence indicates that many of these objects condensed directly from the solar nebula, and have remained relatively unaltered up to the present. Their mineralogical and chemical compositions therefore reflect conditions at the time of their formation. The most thoroughly studied of the inclusions are those from the Allende CV meteorite. These, in general, have mineral assemblages similar to those which would be predicted for nebular condensation. The mineralogical agreement is not strict, however, and also the bulk chemical compositions sometimes deviate markedly from expected trends. More work is required to understand these differences. A range of isotopic anomalies in many elements has been found in these inclusions. Some of these suggest an extra-solar system origin for a part of the material in the inclusions. Although much less work has been done on the inclusions in the CM meteorites, current data indicate that they will prove to be at least as valuable as those from Allende. Chemical data show that some inclusions in the Murchison meteorite are more refractory than the most refractory Allende inclusions. Isotopic anomalies, including ^{26}Mg excesses and oxygen-16 enriched oxygen, indicate that, in spite of chemical and mineralogical differences, the Murchison and Allende inclusions contain common isotopic components, and are probably contemporaneous.

Keywords. Solar system; carbonaceous meteorite; refractory inclusion; mineralogy; chemical composition; isotopic anomaly.

1. Introduction

One of the most important events in the recent history of cosmochemistry occurred on 8 February 1969. That date marks the of fall the Pueblito de Allende CV ($\equiv C3$) chondrite, a meteorite which has probably provided more information about early solar system history than any other. Most of this information has come from detailed mineralogical, chemical and isotopic analysis of the small,

* An invited original paper.

refractory-element-enriched inclusions which occur in Allende. Although similar inclusions had been recognized previously in other CV meteorites, both the size (several tons) and timing (coinciding with improvements in analytical capabilities in anticipation of the Apollo program) of the Allende fall guaranteed that it would be an important sample for inclusion studies.

In this paper we attempt to review briefly some of the more important results which have derived from investigations of Allende inclusions, and then proceed to compare these results with those we have obtained recently from refractory inclusions in the CM ($\equiv C2$) meteorites. The latter have provided a view of early solar system processes that is in some ways different from that obtained from the Allende studies. Although only a limited amount of work has been done on the inclusions from CM meteorites, the results which have been obtained indicate that these objects will be every bit as important in deciphering early solar system events as those from Allende.

2. Inclusions in Allende

2.1. *Classification and mineralogical characteristics*

Like other CV meteorites, Allende consists of an heterogeneous assemblage of inclusions, ranging in size from < 1 mm to several cm, dispersed throughout a very fine-grained dark grey groundmass. Only a small fraction of these inclusions is of the refractory variety; the remainder themselves comprise an heterogeneous collection of objects with diverse origins. Here we will discuss only the refractory variety.

Grossman (1975) devised a simple classification scheme for the Allende refractory inclusions based on their mineralogy. He identified *fine-grained and coarse-grained* inclusions, and sub-divided the coarse-grained variety into two categories, type A and type B. Although subsequent studies of Allende have shown that there are some inclusions which do not fit readily into this classification system, it is nevertheless a useful general scheme, and will be followed here. In table 1 we list the major mineral phases which occur in the various inclusion types, and give an estimate of their abundances. The abundance estimates are taken primarily from Grossman (1980) for the coarse-grained Allende inclusions, Wark (1979) for fine-grained Allende inclusions, and our own unpublished data for the CM meteorites.

It is evident from the data in table 1 that there are considerable mineralogical differences among the inclusion types from a single meteorite class, and also that there are clear differences between CM and CV inclusions. It should be noted that table 1 lists only the major phases generally considered to be primary condensates; especially in Allende inclusions a variety of alkali-rich or otherwise non-refractory phases also occurs. These are believed to have formed at much lower temperatures than the major phases, possibly by reaction with a cool nebular gas. Minerals believed to have been produced by alteration of the primary phases include wollastonite, nepheline and sodalite in Allende inclusions, and calcite and an unidentified iron-rich hydrous silicate in the CM meteorites. As discussed in a later section, an understanding of the alteration process is important for deciphering the isotopic record in these inclusions.

Table 1. Mineralogical make-up of CM and CV refractory inclusions.

Condensation T* (°K)			CV			CM	
			Type A	Type B	Allende fine	Hibonite-rich	Spinel-rich
1750	Hibonite	$CaAl_{12}O_{19}$	≤5	V. low	P	5–85	0
1647	Perovskite	$CaTiO_3$	1–3	..	P	1–10	1–20
?	Fassaite**	$Ca(Mg,Al,Ti)(SiAl)_2O_6$	Low	30–60	..	0–5	0
1625	Melilite	$Ca_2Al_2SiO_7$–$Ca_2MgSi_2O_7$	≥75	5–20	..	0	0
1513	Spinel	$MgAl_2O_4$	5–20	15–30	P	10–80	60–90
1450	Diopside	$CaMgSi_2O_6$	..	..	P	2–5	2–5
1360	Anorthite	$CaAl_2Si_2O_8$	..	5–25	P	0	0

* From Grossman (1972) and Grossman and Clark (1973) for a reference nebula pressure of 10^{-3} atm. In the column for "Allende fine", "*p*", for present, means that this phase is frequently present. Proportions are quite variable in these fine-grained inclusions.
** Condensation temperature unknown. Based on observations by Allen *et al* (1978), fassaite may begin to condense between perovskite and melilite.

Two additional mineralogical features of the Allende refractory inclusions are notable. The first is the presence of thin rims surrounding virtually all coarse-grained inclusions; mineralogically these resemble closely the fine-grained inclusions (Wark and Lovering 1977). The rims are layered, and may represent a sequence of deposition or interaction with the nebular gas. The second is the presence of small refractory metal or metal-rich grains included within the primary minerals of the inclusions (Wark and Lovering 1976; Palme and Wlotzka 1976; Wark and Lovering 1978; El Goresy *et al* 1978). The simplest of these are micron-sized nuggets which are alloys of Pt, Os, Ir, Ru, Rh, Mo, Re and W in approximately chondritic relative proportions. Almost certainly these nuggets are the earliest condensed material in the inclusions, since the refractory metals are predicted to form at higher temperatures than any of the oxide or silicate minerals listed in table 1. More complex refractory-metal-containing bodies also occur in some inclusions. These are often larger than the pure alloys described above, and may contain many separate metal grains with varied abundances of the refractory metals, and also Fe–Ni alloys, phosphates, silicates, sulphides and oxides.

2.2. *Chemical compositions*

In spite of their importance, relatively few major element analyses have been reported for bulk inclusions. In addition, there are analytical problems which may affect the usefulness of some of the published data, as discussed by Grossman (1980). Coarse grain size coupled with small inclusions means that essentially the entire inclusion, free of surrounding matrix, must be analyzed to obtain representative compositional data. Broad beam electron microprobe analyses may give inaccurate results for some elements when applied to small but coarse-

grained objects such as these inclusions. Virtually all whole-inclusion analytical techniques suffer from the problem that secondary or alteration phases contribute to the analysis according to their abundance in the inclusion. Nevertheless, the major element data do give useful estimates of bulk composition. Some representative examples are listed in table 2.

It can be seen clearly from the chemical data that these inclusions are very refractory. Grossman and Larimer (1974) and many other authors have pointed out that, like the mineral assemblages, the major element compositions are approximately those predicted to occur at the high temperature end of the equilibrium condensation sequence, that is, for temperatures above about 1400° K for condensation at 10^{-3} atm. However, as has been pointed out recently by Kerridge (1981), the agreement between prediction and observation is not very precise, and most individual inclusions fall considerably away from the theoretical condensation trajectory when major element ratios are considered. The reason for this discrepancy is not well understood.

Minor and trace element data for the inclusions provide more convincing evidence on the origin of these objects than do major element data. The form in which many of these elements should condense is uncertain, although a few (e.g., some of the platinum group metals) are predicted to form pure metals and others (e.g., Sc, some of the rare earths) should form oxides in the temperature interval represented by the major phases in the inclusions (see Grossman 1973). Indeed, some pure compounds of the refractory trace elements are observed in the Allende inclusions, for example the platinum group metal nuggets mentioned earlier. However, it is likely that many of the trace elements are present in solution in the more abundant phases, and they thus may have condensed at temperatures above those predicted for the pure metal or oxide.

A remarkable feature of the refractory trace element abundances in the coarse-grained inclusions was reported by Grossman and Ganapathy (1976) and

Table 2. Major element compositions for selected Allende inclusion types*.

Oxide wt%	1 Coarse-grained (Fluffy type A)	2 Coarse-grained (type B, average)	3 Fine-grained (average)
SiO_2	25·1	29·6	39·9
TiO_2	1·0	1·3	0·45
Al_2O_3	37·6	28·5	12·8
Cr_2O_3	..	0·05	0·27
MgO	4·3	10·3	17·7
CaO	29·4	28·9	9·7
FeO	1·7	0·76	14·7
Na_2O	0·8	0·36	3·6
K_2O	..	0·01	0·33

* The data are taken from Davis *et al* (1978) for 1, which is a single inclusion, and Wark (1979) for 2 and 3, which are average values.

Grossman *et al* (1977a). These authors measured the concentrations of 20 refractory trace elements, plus calcium, in nine coarse-grained inclusions. In spite of the diverse geochemical properties of these elements, they show a very narrow range of concentrations relative to Cl chondrites, all elements being enriched by a factor between about 15 and 22 times Cl abundances. The mean enrichment factor is 17·5, leading to the conclusion that the inclusions represent approximately 6% of condensable matter (the calculation assumes that these elements are totally condensed in the material making up the inclusions, and thus may be an overestimate). The 20 elements which were measured to obtain this figure are Sr, Ba, Sc, La, Ce, Sm, Eu, Tb, Dy, Yb, Lu, U, Zr, Hf, Ta, W, Re, Ru, Os and Ir.

The rare earth elements (REE) are a special subset of the refractory trace elements, and their relative abundances, normalized to Cl chondrites, are particularly informative. It was noted in the previous paragraph that a number of the REE's show an enrichment in abundance 15–20 × Cl chondrites, similar to other refractory trace elements. However, the REE patterns are distinctive and several characteristic types have been recognized (Mason and Martin 1977; Nagasawa *et al* 1977; Tanaka and Masuda 1973). For the most part these patterns are discussed using the nomenclature developed by Mason and Martin (1977), i.e., Groups I, II, III, etc. Group I REE patterns are common in coarse-grained inclusions and are characterized by approximately uniform enrichments of the rare earths at 15–20 × Cl chondrites except for Eu which usually shows a slight positive anomaly. This has been interpreted (Grossman 1980) as being due to the fact that Eu entered these inclusions as a separate component from that which carried the other REE.

Group II REE patterns are highly fractionated relative to Group I patterns, with approximately uniformly enriched light REE, a negative Eu anomaly, and positive Tm and Yb anomalies superimposed on steadily decreasing relative abundances of the heavy REE. This type of pattern is characteristic of fine-grained inclusions, although it has been found occasionally in coarse-grained varieties. Boynton (1975) has shown that Group II-like patterns would be expected in a condensate formed from a gas from which the most refractory REE had already been partially removed. Until recently this idea remained simply an attractive hypothesis, but with the discovery of an inclusion from the CM meteorite Murchison which exhibits the complementary pattern, the process was confirmed (Boynton *et al* 1980).

Group III REE patterns, which occur predominantly in fine-grained inclusions, are approximately flat, with substantial negative anomalies at Eu and Yb. Other, less common, types of REE patterns are also found in Allende refractory inclusions (e g. see Grossman 1980). Based on theoretical work by Boynton (1975, 1978) and Davis and Grossman (1979), most of the patterns can be understood in terms of several REE components condensed at differing temperatures, and possibly under slightly differing oxidation conditions, with abundances in the individual components controlled predominantly by volatility.

2.3. *Alteration effects*

Many of the inclusions from Allende which have been studied contain secondary phases rich in volatiles and/or alkalis. Examples are wollastonite, nepheline and

sodalite. Frequently these phases line cavities or fill cracks and veins in the inclusions, which have led some workers to believe that they were vapour-deposited (e.g., Allen *et al* 1978). Reaction between inclusion phases and the nebular gas is a scenario consistent with the oxygen isotopic evidence, which indicates that oxygen exchanged with some minerals after their formation (see § 2.4). Details of the inclusion rim mineralogy suggest that at least some of the chemical changes affecting the inclusions occurred after rim formation (Wark and Lovering 1980).

2.4. *Isotopic anomalies*

The important finding that some refractory inclusions in Allende have non-"normal" isotopic compositions was made by Clayton *et al* (1973). These workers measured the isotopic abundance of oxygen in a large number of samples of the anhydrous, "high temperature" fractions of several CM and CV meteorites, including refractory inclusions from Allende, and found compositions deviating widely from those of terrestrial, lunar, chondritic and achondritic samples. Until this discovery it had been widely assumed (based, in part, on reasonably extensive measurements) that the isotopic compositions of elements in all samples of solar system material were constant, except for well-understood variations due to radioactive decay or mass-dependent fractionation in nature. However, the data reported by Clayton and his co-workers showed that heterogeneities in isotopic composition actually do exist in solar system matter, and that mixing of isotopically distinct components was not complete when the Allende inclusions formed. It was also suggested by these workers that the observed oxygen isotopic variations among the Allende inclusions could be due to mixing between normal solar system oxygen, and an exotic, non-solar system reservoir. Only Black (1972) had previously suggested a non-solar system origin for an anomalous isotopic composition (of Ne in some carbonaceous chondrites).

Since the work by Clayton *et al* (1973), isotopic "anomalies" have been found for many elements in a small number of otherwise apparently normal Allende inclusions. Several types of isotopic effects have been distinguished: those due to decay of very short-lived radioactive species, such as ^{26}Al with $t_{1/2} = 0{\cdot}72$ m.y. (Lee *et al* 1976); those related to mass-dependent fractionation, often of much greater magnitude than encountered in terrestrial fractionation (Lee *et al* 1976; Clayton and Mayeda 1977); and those of unspecified nuclear origin, such as the anomalous ^{16}O enrichments originally observed by Clayton *et al* (1973).

A brief discussion of the oxygen isotope data is instructive for understanding the isotopic variations in the Allende inclusions. The range of results for oxygen is shown in figure 1 (after Lee *et al* 1980). The uppermost solid line in this diagram, along which are plotted the points for "blank", terrestrial olivine, etc., has a slope of 0·5, and is defined by all measured terrestrial samples. Data points falling on this line can be understood as representing material which was derived from a single homogeneous oxygen reservoir and subsequently isotopically fractionated. The line AD has a slope of approximately 1·0 and is defined by measurements of Allende inclusions as well as anhydrous silicates and oxides from other CV and CM meteorites. No measurements plot at values of $\delta^{17}O$ or $\delta^{18}O$ lower than about −40. This fact, combined with other evidence to be discussed below, led Clayton and Mayeda (1977) to identify a composition at approximately

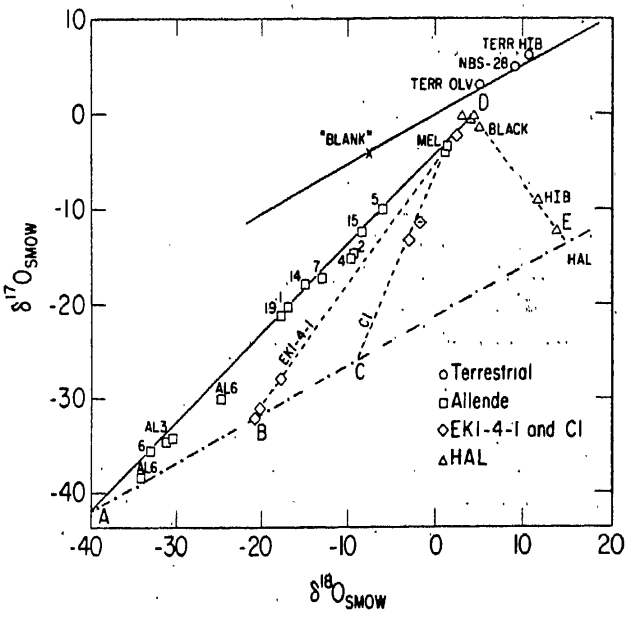

Figure 1. Oxygen isotope plot from Lee *et al* (1980) showing data for Allende inclusions. The upper solid line, with slope 1/2, is the terrestrial trend. Most Allende data plot along AD, suggesting inclusion of a component of essentially pure ^{16}O. Three isotopically peculiar inclusions, EK1–4–1, Cl and HAL plot along the lines BD, CD and ED respectively. Possible reasons for this behaviour are discussed in the text. (Figure reproduced from Lee *et al, Geophys. Res. Lett.* 7 493 1980, copyrighted by the American Geophysical Union.)

point *A* on figure 1 as an end member oxygen component highly enriched in ^{16}O. This component, when mixed with oxygen with a composition represented by D, would explain the observed array of CM and CV oxygen isotope data. Aside from the fact that most measurements on anhydrous phases in CM and CV meteorites plot between A and D on the oxygen isotope diagram, the locations of these presumed end member components are defined by data from three isotopically peculiar Allende inclusions. These are referred to as EK1–4–1, Cl and HAL, and measurements on mineral separates from these objects fall along the three dashed lines labelled BD, CD and ED in figure 1. The line AE was drawn through the data points for spinel from inclusion EK1–4–1 and the inclusion samples fall on the mixing line AD which have the most highly ^{16}O-enriched compositions (these are also spinels). The line AE has a slope of approximately 0·5, as would be expected for simple mass-dependent fractionation. Clayton and Mayeda (1977) interpreted the oxygen isotopic data for EK1–4–1 and Cl as being due to (i) mass-dependent fractionation of oxygen from a reservoir with the characteristics of A, resulting in composition B or C, which was the initial oxygen isotopic composition of all phases in EK1–4–1 or Cl, respectively; and (ii) subsequent back reaction, including oxygen exchange for some minerals, with a more "normal" nebular gas in which oxygen had a composition represented by point D. During the back reaction step, spinel was resistant to oxygen exchange, while melilite was strongly

affected. Obviously alteration-produced phases, such as alkali-rich minerals, also plot near D. Data from the inclusion HAL are consistent with such a model (Lee *et al* 1980).

Although the sequence of events described above seems to fit the data quite well, the nature of the reservoirs represented by A and D is unknown, as is the mechanism required to bring about the highly fractionated compositions of the starting materials for the three inclusions at B, C and E. The inclusions EK1–4–1, C1 and HAL have been found also to exhibit fractionation and nuclear effects in a number of elements other than oxygen (e.g., Clayton *et al* 1978; Yeh and Epstein 1978; Lee *et al* 1979a; Lugmair *et al* 1978; McCulloch and Wasserburg 1978a, b; Papanastassiou and Wasserburg 1978). It appears that large fractionation effects in oxygen are usually accompanied by fractionation effects in other elements (e.g., Mg, Ca, Si) *and* by a variety of " nuclear " effects in some elements (e.g., Sr, Nd, Sm, Ba, Si, Mg, Ca). The correlation between these two types of anomalies has led to their designation as FUN (fractionation and unknown nuclear) anomalies. A reasonably complete discussion of these anomalies was given recently by Lee (1979), and will not be repeated here. However, the presence of isotopic anomalies of several types for a variety of elements in a few rare (but mineralogically unremarkable) Allende inclusions implies a connection among the causes of the anomalies, and makes these objects very important for studying early solar system processes.

2.5. *Major implications of the Allende data*

The mineralogical compositions of the refractory Allende inclusions leave little doubt that they are samples of early condensed material. The mineral assemblages observed, particularly in the coarse-grained type A inclusions, are almost identical to those predicted to form from a gas of solar composition during equilibrium condensation (Grossman 1972; Lattimer and Grossman 1978). The actual mechanism of formation of the inclusions is speculative, and several possibilities have been suggested. Some of the arguments are based primarily on textural evidence. For example, a number of authors have postulated that the compact varieties of coarse-grained inclusions formed by crystallization from a liquid (e.g., Mason and Martin 1974; Mason 1975; Blander and Fuchs 1975; MacPherson and Grossman 1979). On the other hand, MacPherson and Grossman (1979) suggested that " fluffy " type A inclusions were formed by aggregation of condensed grains. The inclusions may also have condensed directly from the gas to form either compact or " fluffy " inclusion types.

All these modes of formation are compatible with a condensation origin for the inclusions. It has been suggested by some (e.g., Kurat *et al* 1975; Chou *et al* 1976) that volatilization and evaporation processes are of major importance in producing the refractory compositions; however, arguments based on trace element abundances (Grossman 1980) and REE patterns (Boynton 1975) appear to contradict this possibility for the majority of inclusions. In particular, the Group II patterns discussed by Boynton (1975) and described in an earlier section seem to rule out an evaporation step for the REE component.

If the equilibrium condensation calculations given by Grossman (1972), with later revisions by Grossman and Clark (1973) and Lattimer and Grossman (1978),

can be applied to Allende, then the inclusions represent condensation products formed over a relatively high, and relatively narrow, range of temperatures, i.e. 1533–1438° K for an assumed pressure of 10^{-3} atm. Increased pressure would permit formation at higher temperatures, but over a range of several orders of magnitude in the neighbourhood of 10^{-3} atm, the condensation curves for the major phases are effectively parallel, so that the *sequence* of phases would not change. Thus falling pressure could as well be responsible for the observed mineral sequences as falling temperature (the case usually assumed).

The central portions of most inclusions do not show a well-defined or layered sequence of phases as might be expected under ideal conditions of condensation. Instead, phases are intergrown in approximately random fashions suggesting essentially simultaneous growth, or aggregation and continued growth after initial formation. However, the outer rims do exhibit a distinct stratigraphy (Wark and Lovering 1977). The individual layers of these rims are considered by some workers to be markers, recording changes in the external environment in which the inclusions were forming (Wark and Lovering 1977). At least some of the phases present in the rims are not predicted as condensates, which may imply that part or all of the rim sequences were produced by reaction mechanisms between the inclusion core and an uncharacterized surrounding medium. Since rim sequences do not exist on obviously fragmented inclusion surfaces, it is clear that their formation did not occur by reaction with matrix material. They must thus predate aggregation of the meteorite to its present form. The rims on a particular inclusion type exhibit a fairly reproducible sequence of phases, but the sequence varies from one inclusion type to another. This suggests that either the substrate (i.e., the core of the inclusions) was important in determining the mineralogy of the rims, or that each inclusion type acquired its rims under different conditions. If the rims are condensation products, then their formation temperatures must have been quite high, since they contain many of the same refractory phases found in the inclusion cores (e.g., hibonite, titanium pyroxene, diopside). However, refractory phases sometimes overlie less refractory minerals such as sodalite and nepheline, so that the simple picture of equilibrium condensation in a smoothly decreasing temperature regime is not applicable. In a recent re-examination of inclusion rim sequences, Wark and Lovering (1980) concluded that some of the apparent inconsistencies in the sequences might be secondary rather than primary features. Nevertheless, the rims are still rather enigmatic, and require further detailed work before their full store of potential information can be extracted.

The isotopic characteristics of the Allende inclusions also require considerable further study before their full bearing on the history of these objects is understood. The presence of ^{26}Al in some of these inclusions at the time of their formation, reflected in the present-day ^{26}Mg excesses discussed earlier, implies formation very shortly after incorporation of newly synthesized material into the solar system. The limited data from Allende imply that $(^{26}Al/^{27}Al)_0$, the parent-to-daughter ratio at the time of inclusion formation, was in the neighbourhood of 5×10^{-5}, although both lower (Lee *et al* 1976, 1979a; Esat *et al* 1978) and possibly higher (Lorin and Christophe Michel-Levy 1978) values have been reported. A major unanswered question is whether these variations reflect time differences or isotopic heterogeneity. The time differences that would be required

to explain the observed variations among inclusions amount to several millions of years, much longer than would be expected for the cooling nebula. Thus the resolution of this question is an important one. Experimentally the problem is difficult but within the present analytical capabilities. For example, measurement of precise internal isochrons in the Al–Mg system for a series of inclusions might provide the required data.

Although there is some ambiguity about the cause of $(^{26}Al/^{27}Al)_0$ differences from inclusion to inclusion, there is clear evidence for isotopic heterogeneity for a number of other elements not affected by radioactive decay. As mentioned earlier, one of the most striking of these, and the first discovered, is oxygen. As far as is known based on presently available data, the oxygen isotopic heterogeneities are unique in that they are observable not only in refractory materials from carbonaceous chondrites, but extend to a planetary scale. The earth and various classes of meteorites define a series of parallel fractionation lines on the oxygen isotope plot, suggesting that each of these categories of material formed initially from matter with different average oxygen isotopic composition (Clayton *et al* 1976). It seems likely that these differences result from mixtures of end member components along the line AD (figure 1) and its extension. Even if one of the end members, presumably with normal solar system oxygen isotopic composition, predominates in these mixtures, rather large amounts of material with the anomalous composition are required to explain the observed shifts. This is so because oxygen is a major element.

Except for the noble gases, which have not been discussed here, the anomalies in elements other than oxygen have so far been detected only in refractory inclusions, predominantly, although not exclusively, of the FUN type mentioned previously. Although in general anomalies in most elements in most inclusions can be explained in an *ad hoc* way by invoking incorporation of material with a particular nucleosynthetic signature, there has been no satisfactory synthesis which can explain the data for all elements in an integrated way. However, it is clear that especially the FUN inclusions contain varying amounts of one or more components of matter which do not have the average solar system isotopic composition. A major goal of most isotopic studies of these inclusions is to unravel the nature of this component (or components) and discover its origin and mode of incorporation into the Allende inclusions.

The fact that the ^{16}O-enriched component is most abundant in the refractory materials from carbonaceous chondrites suggests that it may be linked with the other isotopic anomalies found only in these inclusions. However, the magnitude of the oxygen effect is much greater than those found for other elements, so it seems likely that more than one component is involved. At least one of these must have been created shortly before the beginning of condensation, otherwise evidence for live ^{26}Al would be lacking in the Allende inclusions. Considering the nature of the anomalies, many workers have suggested that the anomalous component represents extra solar system material produced in a supernova and incompletely mixed into the solar system. The short time scale implied by the presence of live ^{26}Al at the time of formation of some inclusions may require that the supernova exploded close to the solar system. Such speculations have stimulated a great deal of astrophysical research in recent years (e.g. Clayton 1977;

Falk *et al* 1977; Cameron and Truran 1977; Consolmagno and Cameron 1979; Lattimer *et al* 1978; Lee *et al* 1979b; Margolis 1979).

3. Inclusions in the CM meteorites

Until very recently, little work had been carried out on the refractory inclusions in the CM (≡C2) meteorites. This was probably due to their small size (typically < 1 mm), their relative rarity, and the small amounts of CM material available for study. However, several recent studies have indicated that these inclusions may be especially interesting (Macdougall and Phinney 1979; Boynton *et al* 1980; Grossman *et al* 1980), and considerable effort is now being expended in unravelling the details of their history.

Fuchs *et al* (1973) first described the calcium-aluminium rich inclusions which occur in Murchison as part of their general petrographic and chemical study of that meteorite. A more detailed examination of the refractory inclusions in CM's was published by Macdougall (1979).

3.1. *Mineralogy and texture*

Among the important features of the CM inclusions is their distinctness from those found in the CV meteorites such as Allende. In spite of the fact that a number of the same phases occur in CM and CV inclusions, the overall mineralogical make-up in the two cases is quite different (table 1). Although distinct from the CV inclusions, those in the CM's are very similar from meteorite to meteorite. We have examined essentially identical types of inclusions in Murchison, Murray, Mighei, Cold Bokkeveld, Nogoya and Santa Cruz, and have seen similar inclusions in more preliminary studies of Banten.

The chemically most refractory inclusions in the CMs can be grouped into two general classes based on the presence or absence of hibonite. Both hibonite-bearing and non-hibonite-bearing inclusion types have irregular, often convoluted, outlines, contain substantial void space, and are relatively fragile (figures 2 and 3). Both varieties usually contain very pure magnesian spinel as the major phase, although in a small number of the several hundred inclusions we have examined hibonite is the major phase. Occurrence of corundum was found only in a single spinel-rich inclusion in Murray. Nearly all inclusions are completely rimmed by a fine-grained (2–5 μm) diopside layer, usually not more than one or two crystals thick. Most of the refractory inclusions also contain perovskite. Most frequently the perovskite is poikilitically enclosed in spinel, very occasionally in hibonite, and sometimes it occurs as individual crystals independent of these phases. Consistent with its position in the condensation sequence, perovskite is usually concentrated in the interiors of inclusions, although in rare cases we have observed a band of perovskite rimming inclusions immediately inside the diopside layer (e.g., see figure 4). The small size of the perovskite crystals has precluded accurate microprobe analyses for comparison of interior and rim perovskite. A further feature of most of the CM inclusions is the presence of a well-defined layer of what appears to be a secondary iron-rich hydrous silicate (figures 2 and 4). Some representative analysis of phases from CM inclusions are given in table 3.

Table 3. Representative mineral analyses from refractory inclusions in CM meteorites.

	1	2	3	4	5	6	7	8	9
MgO	3·56	2·83	0·59	27·4	26·6	27·4	18·0	18·3	6·66
Al_2O_3	78·9	82·1	90·2	71·2	72·1	71·9	9·76	1·45	4·48
SiO_2	0·23	0·28	0·09	..	0·08	0·05	47·0	54·9	23·5
CaO	8·53	8·33	8·25	0·08	0·24	..	22·0	23·9	0·14
TiO_2	7·62	5·10	1·26	0·28	0·18	0·82	0·94	0·50	0·14
Cr_2O_3	0·08	0·06	0·04	0·06	0·08	0·15	0·16	0·52	..
FeO	0·24	0·32	0·05	0·13	0·47	0·05	0·72	1·07	50·5
Total	99·16	99·02	100·48	99·15	99·75	100·37	98·58	100·64	85·42

1. Hibonite, Murchison inclusion MTS4–4; 2. Hibonite, Mighei inclusion MITS–1; 3. Hibonite, Murray inclusion MY6–1; 4. Spinel, Murchison inclusion MT52–25; 5. Spinel, Murray inclusion PTSKF–C; 6. Spinel, Murchison inclusion MH123; 7. Diopside, Murchison inclusion MTS4–4; 8. Diopside, Murchison inclusion MH28A; 9. Fe-rich silicate band in Murchison inclusion MCl–N.

The convoluted, fragile inclusion types described above cannot be extracted as entities from the matrix without fragmenting. However, there are analogs of both hibonite and non-hibonite-bearing varieties which occur as coherent spherules or chondrules. In these, spinel is a major phase, perovksite is usually poikilitically enclosed in spinel, and, in most cases, the spherule is rimmed by an outer diopside layer surrounding an iron-rich silicate band (figure 5). For both the irregular inclusions and the compact spherules, hibonite-bearing varieties are in the minority, and comprise on the order of only 10% of each type of refractory inclusion.

Electron microprobe analyses of spinel, hibonite and diopside show that the chemical compositions of these phases are essentially the same in both the irregular inclusions and the spherules, although fewer data are available for the spherules since they constitute only about 0·1% of the CM refractory inclusions. Spinel is invariably very pure, with Cr_2O_3, FeO, TiO_2 and CaO present at levels less than ~ 0·5%. Hibonite has a wide compositional range, even within the same inclusion. Al_2O_3 varies inversely with (MgO + TiO_2), and ranges from approximately 77 to 91%. Some of these features are shown graphically in figure 6. Although the most aluminous hibonite should condense first, we have not observed any correlations between hibonite composition and position of the crystals within individual inclusions. Among the refractory trace elements we have attempted to measure in hibonite with the electron microprobe, Sr and Zr are below detectability limits (~ 200 ppm) while Sc ranged between 200 and 500 ppm, and V between 0·03 and 0·16%. Others (e.g., Armstrong *et al* 1980) have reported higher and more variable V contents for some Murchison hibonite.

The outer rim diopside in most inclusions is quite pure. In a few cases Ti- and Al-bearing pyroxenes also occur near the rim, usually grading to pure diopside

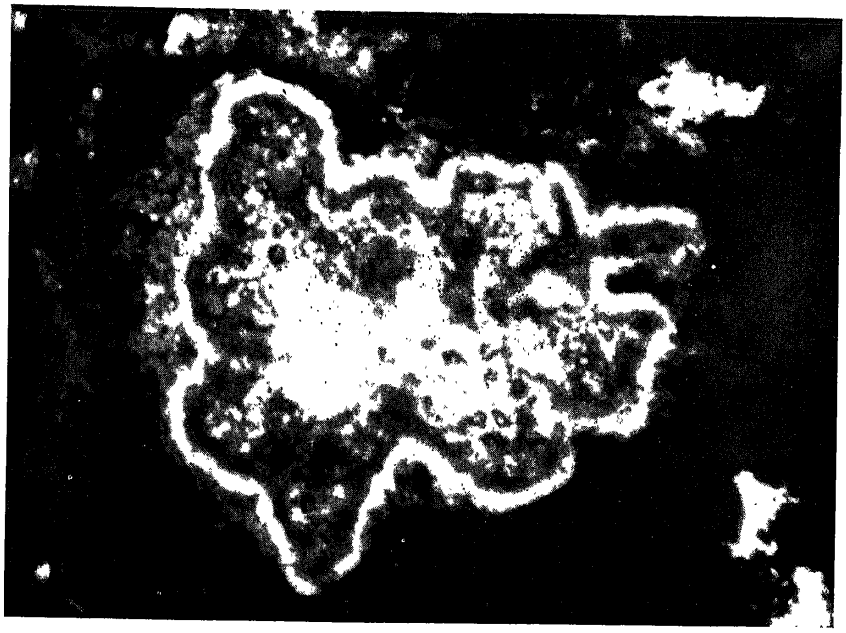

(a)

(b)

Figure 2. Transmitted light photomicrographs of refractory inclusions in Murchison thin sections. Note the convoluted shapes and the distinctness of the outer diospide layer (light colored) and the iron silicate layer (dark). The background is dark for these photographs because of the opaqueness of the fine-grained matrix. (a) Inclusion MTS 3-8. The width of field is 290 μm. The white patch in the central part of this inclusion is $CaCO_3$. (b) Inclusion MTS4-2. Width of field is 290 μm.

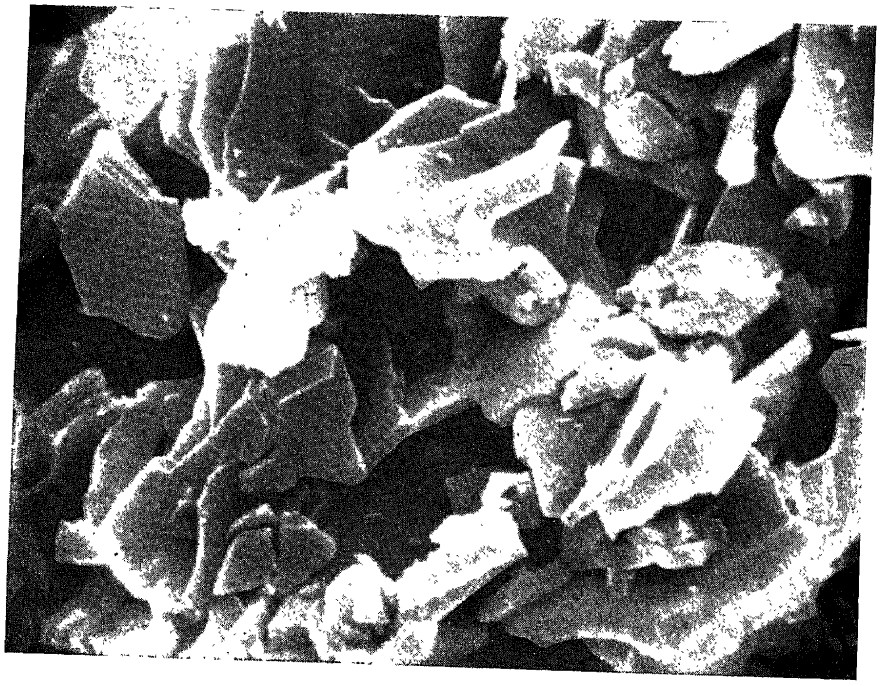

(a)

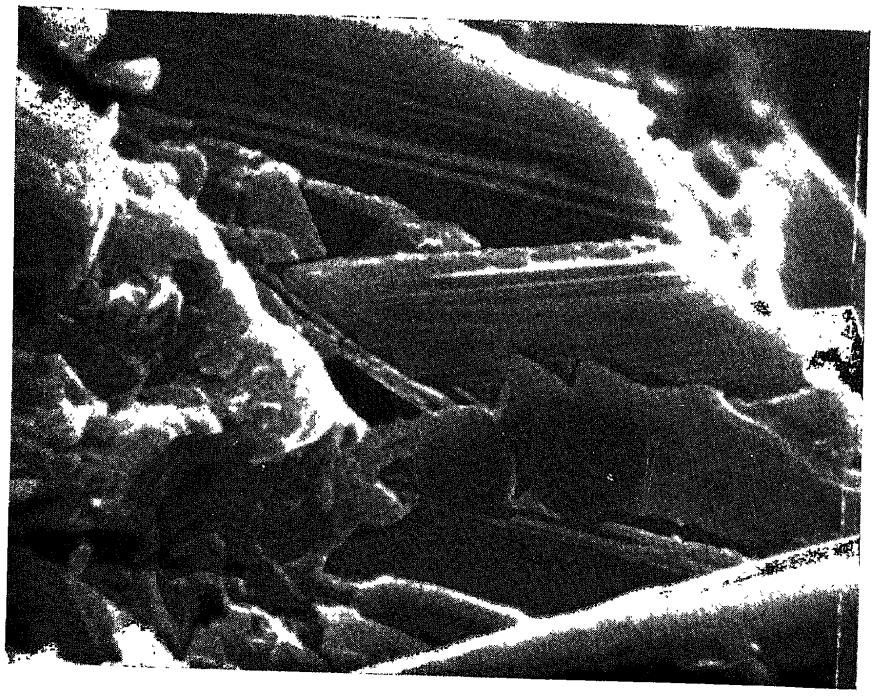

(b)

Figure 3. Scanning electron microscope images of the interiors of two Murchison refractory inclusions. The inclusions were broken open, gold coated, and examined. (a) Murchison inclusion MH–10. All crystals in the photograph are hibonite. Note the fragile, void-filled nature of this inclusion. Small rounded mounds on some crystals are artifacts of the gold coating procedure. The field of view is 24 μm across. (b) Murchison inclusion MH115. The striated crystals are hibonite, the smooth-surfaced saw-tooth edged crystal in lower center is spinel. Note that the spinel appears to be growing at the expense of the hibonite, since it cuts across the surface striations. The field of view is 21 μm across.

Figure 4. Scanning electron microscope image of Murray inclusions PTSKF-F showing details of the complex diopside-perovskite-iron silicate rim. Field of view is 90 μm.

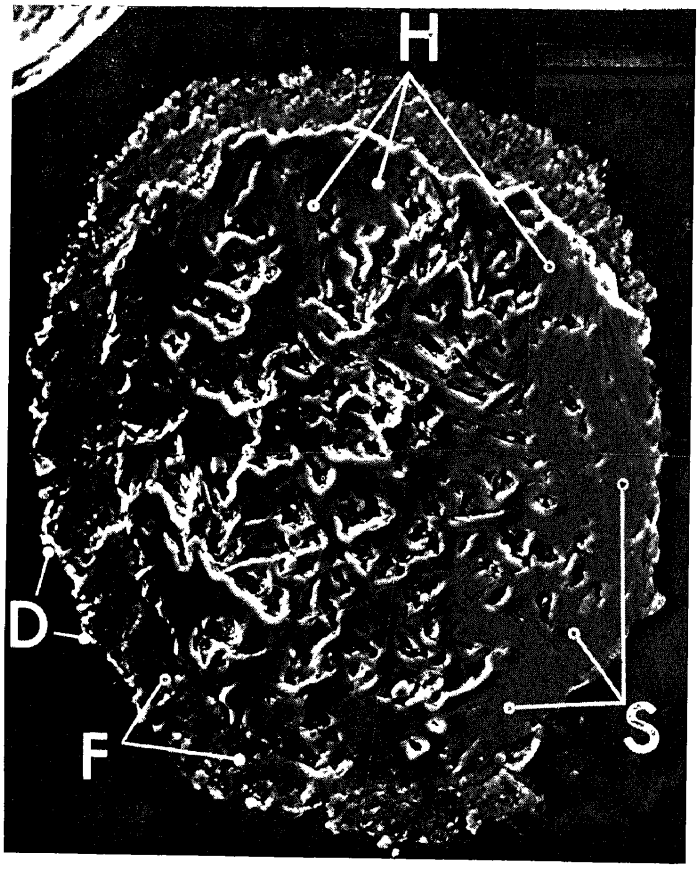

Figure 5. Scanning electron microscope composite photograph of a polished section of a refractory spherule from Murchison. Hibonite (H), spinel (S), iron-rich silicate (F) and diopside (D) are present in this example. The diameter of this spherule is 170 μm.

at the inclusion border. In one fine-grained hibonite-spinel inclusion we observed large, purplish fassaite crystals with TiO_2 up to almost 17% (Macdougall 1979).

Texturally, the irregular inclusions are "fluffy", with considerable void space. Crystals are generally anhedral to subhedral, with hibonite occurring as very thin laths and both spinel and diopside as approximately equidimensional grains. Hibonite and spinel are sometimes intergrown, the usual relationship being that spinel appears to enclose or partially surround hibonite laths. In a few instances, there are textural indications that spinel has partly replaced hibonite (figure 3b) as would be expected from the equilibrium condensation sequence.

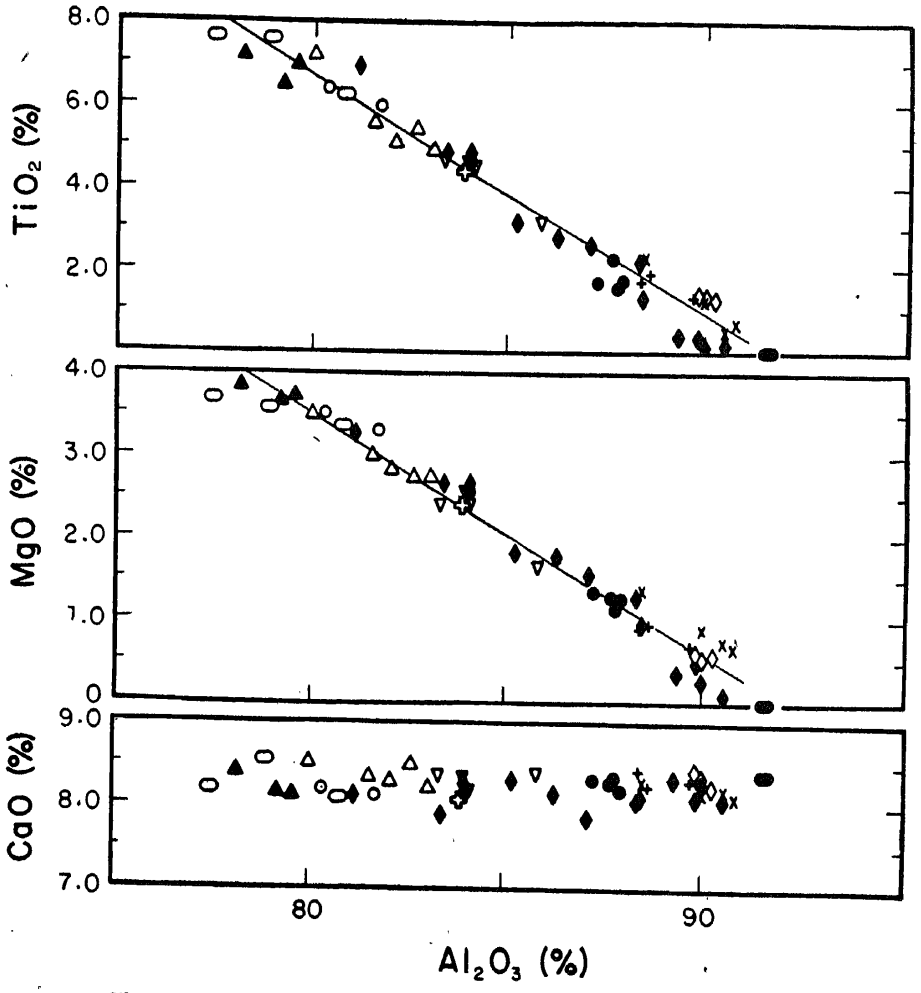

Figure 6a.

Figure 6. Graphical presentation of selected analytical data for Murchison, Mighei and Murray hibonite (**6a**) and Spinel (**6b** and **6c**). Different symbols represent different inclusions. In 6a we show hibonite analyses. It can be seen that there is a considerable compositional range even within a single inclusion. The filled oval is the ideal hibonite composition, $CaAl_{12}O_{19}$. Solid lines are regression lines drawn through the data points. **6b** and **6c** show minor element variations in spinel. For the refractory trace elements (Ca, V and Ti) there are weak positive correlations.

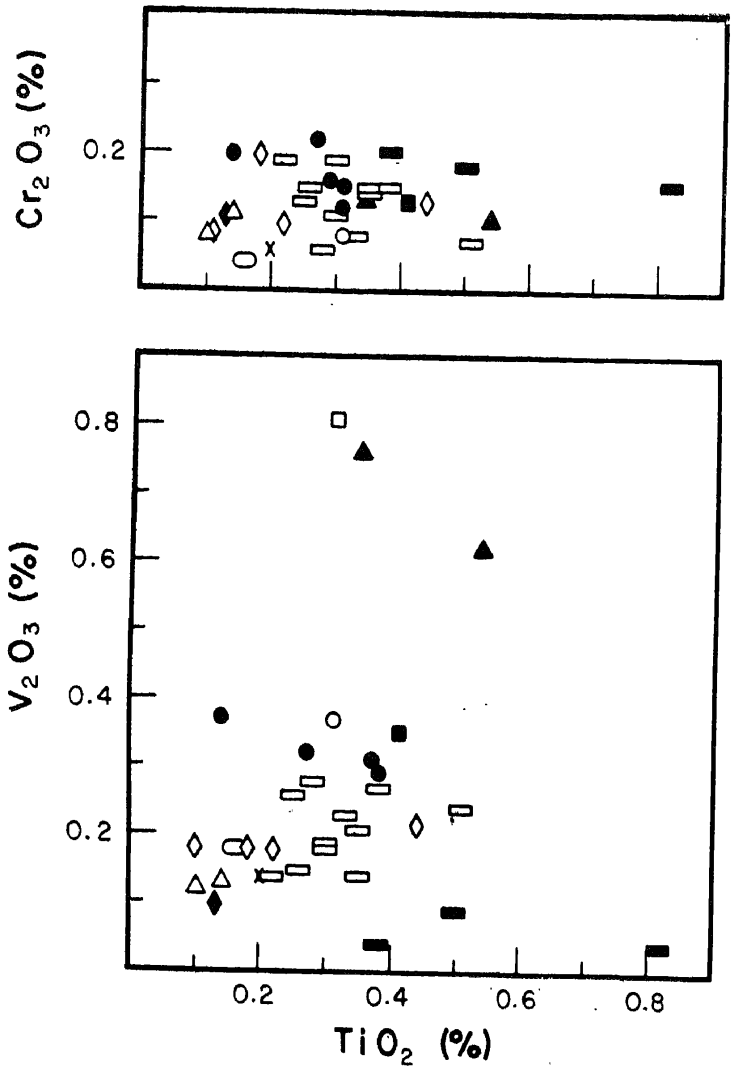

Figure 6b. See caption in p. 17.

In contrast to the irregular inclusions, the compact spherules contain much less void space. Most have central regions which are roughly spherical and composed entirely of spinel with small included blebs of perovskite. A few that we have examined contain hibonite laths within the spinel. The textures in these are igneous-like. In figure 5 we show one of the hibonite-bearing spherules in which the hibonite laths appear to radiate inward from the exterior edge of the inner core, as might be expected if the spherule crystallized from the molten state. However, the concentric banding of the Fe-rich silicate and diopside rims are not consistent with crystallization from a liquid, and imply that at least these phases were later additions to the solid spherule, either by reaction or direct condensation.

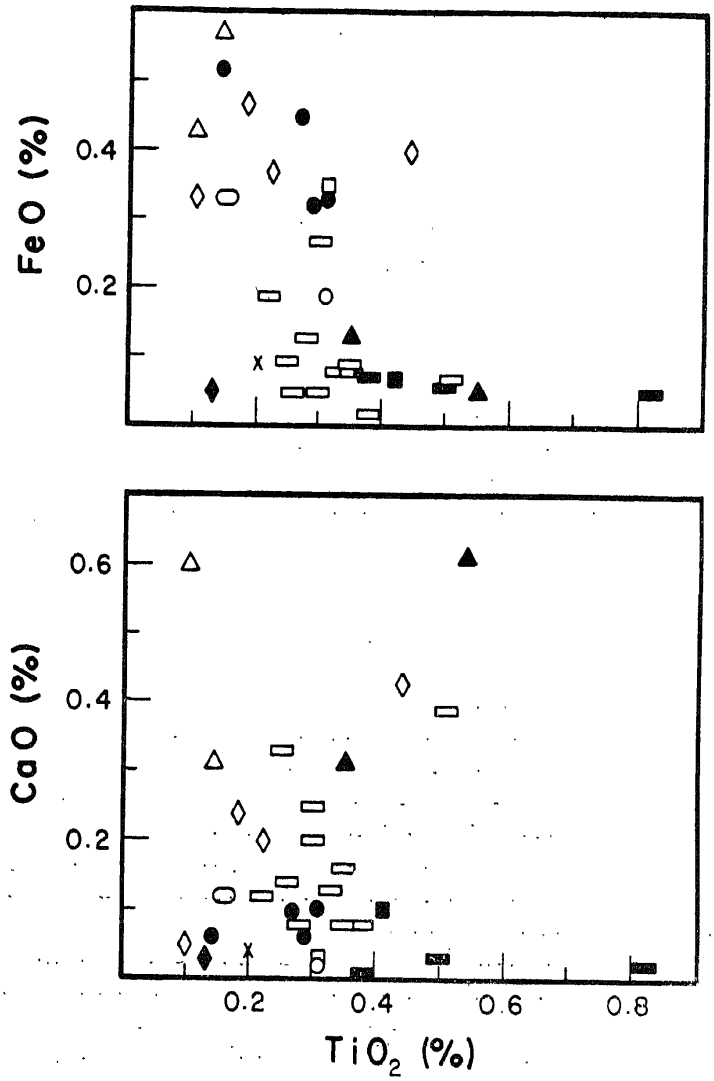

Figure 6c. See eaption in p. 17.

A notable feature of both the spherules and irregular inclusions in the CM meteorites is the lack of refractory metal nuggets of the type found in Allende and discussed earlier. We have searched for these objects extensively in CM inclusions, and have found none. Bar Matthews *et al* (1980) reported "rare noble-metal nuggets" included in spinel or fassaite in Murchison spinel-pyroxene aggregates which may be similar to the diopside-rimmed spinel inclusions discussed here.

3.2. *Chemical composition*

The bulk major element compositions for the Murchison inclusions are quite different from those of most Allende inclusions. Macdougall (1979) estimated

the following composition for "average" hibonite-bearing inclusions from Murchison: Al203 = 67·2%, MgO = 20·7%, CaO = 5·5%, TiO_2 = 5·5%; SiO_2 = 1·1%. The very high Al content is noteworthy, and suggests that these inclusions have "frozen in" a composition corresponding to a very early stage of the condensation sequence. The recent discovery of a corundum-bearing inclusion in Murchison (Grossman *et al* 1980) seems to confirm this view. The corundum forms the inclusion core, and is surrounded by hibonite with small amounts of interstitial perovskite. No spinel occurs in this inclusion; its bulk composition is approximately 91·3% Al_2O_3, 6·5% CaO, 0·5% MgO, 1·7% TiO_2, based on the data given by Grossman *et al* (1980). Thus it appears that the refractory-enriched inclusions in the CM meteorites provide a series of "snapshots" of the early condensation sequence, with the corundum-bearing inclusions representing the high temperature and the spinel-perovksite inclusions representing the low temperature end of the represented spectrum. In spite of this mineralogical and compositional range, virtually all of the CM refractory inclusions observed *in situ* are rimmed with a thin diopside layer, as discussed earlier. (The corundum-bearing inclusion described by Grossman *et al* (1980) was not reported to have such a rim. However, it was separated from the matrix by a rather violent freeze-thaw procedure, which probably would have removed such a layer, if indeed it was originally present). Thus, regardless of differences in prior history, nearly all of the refractory inclusions seem to have experienced the diopside deposition phase.

A major compositional difference between the CM and Allende inclusions is the low Si contents of the former. Mineralogically this is reflected in the lack of silicates in the CM inclusions, and the presence of melilite or pyroxene as a major component of the Allende inclusions. The CM inclusions also have considerably higher Mg and lower Ca contents than most Allende inclusions. The bulk compositions of most CM inclusions are quite different from predictions based on the equilibrium condensation sequence, and must reflect a fractinnation step at some point in their history.

Very few data are available for trace elements in the CM inclusions. Grossman *et al* (1977b) analyzed by neutron activation a combined sample of two hibonite-bearing samples from Murchison. They found enrichments relative to chondrites ranging from about 7 × (for Ir) to 50 × (for the light rare earths) for 17 refractory elements. As in the case of Allende coarse-grained inclusions, the enrichment occurs for both lithophile and siderophile elements. The REE pattern for the combined sample is similar to those found in the type II Allende inclusions discussed earlier.

In contrast to this relatively normal REE pattern for the inclusions examined by Grossman *et al* (1977b), Boynton *et al* (1980) reported a Murchison hibonite-bearing inclusion which appears to contain an ultra-refractory rare earth element component. The REE pattern for this inclusion shows a strong enrichment in the heavy rare earths, with large anomalies at Eu and Yb and smaller anomalies at Ce and Tm (figure 7). Just such a pattern was predicted by Boynton (1975) to be present in the first REE-containing solids to condense from the cooling solar nebula. As mentioned in an earlier section, Boynton pointed out that the typical Allende Group II REE patterns could be produced by prior removal of an ultra-refractory REE component, although a component with the requisite abundance pattern has never been found in Allende. The data for Murchison inclusion

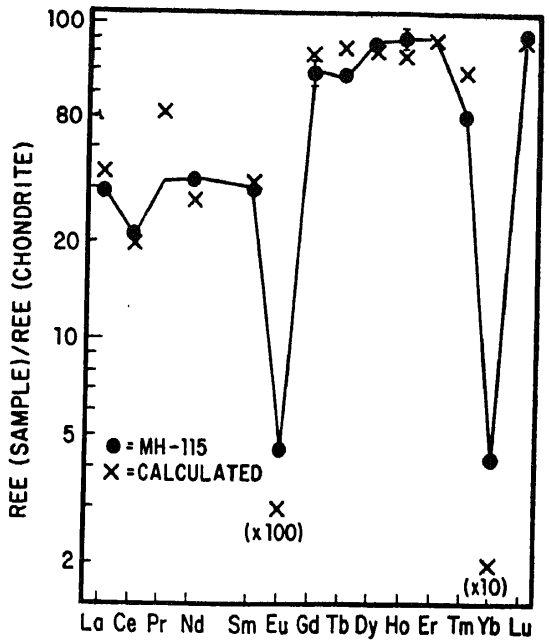

Figure 7. The REE pattern of Murchison inclusion MH-115, compared with values expected for the refractory complement of the rare earths from Allende Group II inclusions (Boynton 1975). This figure is from Boynton *et al* (1980). (*Lunar Planet. Sci.* XI, p. 103, Lunar Planet. Inst., Houston.)

MH115 seem to match the required abundances well (figure 7). The very high enrichments of the most refractory elements, by approximately a factor of 100 relative to chondrites, imply that the material in this inclusion is representative of about the first 1% of condensable matter formed in the solar system.

An interesting feature of the trace element characteristics of the Murchison inclusions is the high abundance of refractory siderophile elements such as Ru, Ir and Os. Although these elements are not as highly enriched as some other refractories in the combined inclusion sample measured by Grossman *et al* (1977b), they are all within a factor of 2 of their abundances in average Allende coarse-grained inclusions (Grossman *et al* 1977a). This is in spite of the fact that, as indicated earlier, refractory metal nuggets such as are found in the Allende inclusions are apparently absent in Murchison. This implies that these elements are instead dissolved in other phases, and thus that the conditions of condensation for these elements were quite different for CM *vs.* CV meteorites.

3.3. *Alteration effects*

In general, the CM refractory inclusions do not appear to have been as strongly affected by secondary processes as those from the CV meteorites. This is also true of the meteorites as a whole. Nevertheless, the secondary phases in the CM inclusions seem to reflect a complex alteration sequence. First, there is the ubiquitous green phase, labelled "spinach" by Fuchs *et al* (1973). This phase occurs in some, but not all, inclusions, and its abundance correlates roughly with

the overall state of alteration of the meteorite. However, there is considerable variation, on a mm scale, in the development of this phase, indicating that its production did not involve a pervasive event after the meteorite components had been assembled into their present configuration. Distinguishable from the spinach phase, both by its mode of occurrence and by differences in chemical composition, is a yellow-brown phase which occurs in virtually all CM refractory inclusions (see figures 2 and 4). This iron-rich silicate phase forms a distinctive band near the inclusion edge, normally just inside the outer diopside layer. On its inner edge, it abuts against spinel. Even in the most convoluted inclusions the iron-rich band follows the inclusion outline faithfully. Generally the Fe silicate layer is thin, $< 10\,\mu m$. Microprobe analyses (table 3) show it to be very iron-rich, and the low totals suggest that it is hydrous. It is evident from fragmental inclusions, in which the band ends abruptly at broken edges and unaltered spinel is in direct contact with matrix, that the iron-rich silicate layer did not form *in situ* by reaction with matrix components. The hydrous silicate is clearly secondary but whether it had a precursor phase not-now-represented in the inclusions is unknown. Interestingly, Fe metal should condense in the temperature interval between diopside and spinel. It is conceivable that the iron silicate layer was, formed during a short duration, low temperature episode when the inclusions were still independent objects.

Although the CM inclusions do not exhibit the alkali enrichments found in CV inclusions, they do occasionally contain calcite (see figure 2). Texturally, the calcite often appears to occur as a cement filling voids in the interiors of the "fluffy" inclusions. One large inclusion we observed in a Murchison thin section was composed predominantly of calcite, which occupied the entire core of the inclusion. The calcite enclosed perovskite and spinel crystals, and was surrounded by a discontinuous Fe-silicate band and an outer diopside layer. The calcite is quite pure $CaCO_3$. The textural evidence from the inclusions, and the fact that calcite occurs intergrown with matrix phyllosilicates, suggests that it was deposited from liquid water. It was probably one of the latest phases to form, possibly during or after the final agglomeration of the meteorite components.

3.4. *Isotopic anomalies*

Only a small number of isotopic analyses have been carried out on CM refractory inclusions. The few published results all deal with Mg isotopic composition, and concentrate on hibonite. The scarcity of isotopic work is mainly due to the very small size of these inclusions: with present techniques there is simply not enough material in most CM inclusions to permit high precision measurements for many elements. The Mg isotope studies have been done either by ion microprobe (Macdougall and Phinney 1979; Tanaka *et al* 1980; Hutcheon *et al* 1980) or by direct loading of small crystals onto the mass spectrometer filament (Papanastassiou and Wasserburg 1980). No oxygen isotopic analyses have been made directly on CM inclusions, but anhydrous mineral separates from these meteorites show ^{16}O enrichments similar to those observed in Allende inclusions.

The first Mg isotope analyses to be made on CM inclusions were reported by Macdougall and Phinney (1979). These authors identified a series of interesting effects in Murchison hibonite crystals, including the largest mass fractionation ever

observed for Mg, $\approx 10\%$ per mass unit, small ^{26}Mg excesses possibly due to ^{26}Al decay, and apparent isotopic variability within individual crystals. They also identified hibonite crystals with relatively high Al/Mg but isotopically normal Mg, implying differences either in the time of formation or in the initial $^{26}Al/^{27}Al$ for the Murchison inclusions. A summary of their data is shown in figure 8.

The large fractionation effects were found in a small inclusion composed almost entirely of relatively coarse-grained hibonite. Electron microprobe analyses of crystals from this inclusion showed considerable variation in magnesium content, from about 0·34% to 2·2% MgO. The two areas analyzed by ion microprobe for isotopic composition differed in $^{27}Al/^{24}Mg$ by a factor of 1·5 and appeared to show corresponding variation in the degree of mass fractionation. This suggests that the Mg in these hibonites is a mixture of at least two isotopically distinct components, one fractionated and one normal. The fractionated end member appears to be associated with relatively low Mg concentrations. It is possible that the observed isotopic composition is the result of partial equilibration of fractionated and normal Mg components after grain formation, analogous to the postulated cause of oxygen isotopic variations observed in Allende inclusions (Clayton and Mayeda 1977; Wasserburg *et al* 1977).

The ^{26}Mg excesses reported by Macdougall and Phinney (1979) could not be correlated with Al/Mg within the relatively low levels of precision of their technique. However, assuming the excesses to be due to *in situ* decay of ^{26}Al, $(^{26}Al/^{27}Al)_0$, the initial aluminium isotopic ratio, would be in the neighbourhood of that deduced for a number of Allende inclusions, i.e. about 5×10^{-5} (Lee *et al* 1976; Lee *et al* 1977). Subsequent investigations have confirmed the presence of ^{26}Mg excesses in some Murchison hibonite (Hutcheon *et al* 1980; Papanastassiou and Wasserburg 1980) and in melilite from two apparently unique melilite-bearing inclusions from Murchison (Tanaka *et al* 1980). In all cases where ^{26}Mg excesses were observed, the data imply that $^{26}Al/^{27}Al$ was 5×10^{-5} at the time of inclusion formation. This ratio is deduced not only from individual data points, but also from isochrons defined by data from several inclusions (Tanaka *et al* 1980; Hutcheon *et al* 1980). If the ^{26}Mg excesses are interpreted to have chronological significance, this result means that these Murchison inclusions were formed contemporaneously with some Allende inclusions. However, Tanaka *et al* (1980), Hutcheon *et al* (1980) and Macdougall and Phinney (1979) also report hibonites with relatively high Al/Mg but no ^{26}Mg excess. These may reflect differences in $(^{26}Al/^{27}Al)_0$ among the Murchison inclusions. For the similar but much more extreme case of the unique Allende inclusion HAL, Lee *et al* (1979a; 1980) have argued that the lack of a ^{26}Mg excess in spite of very high Al/Mg may be due to exchange of initially ^{26}Mg-enriched magnesium with normal Mg in the solar nebula after ^{26}Al decay was complete. Particularly for the Murchison inclusions, this is a problem deserving much more study. Mg isotopic data still hold the promise of providing chronological information for these objects.

4. Summary of the CM data

Like the Allende refractory inclusions, those from the CM meteorites provide a window on early solar system processes. Their chemical, mineralogical and iso-

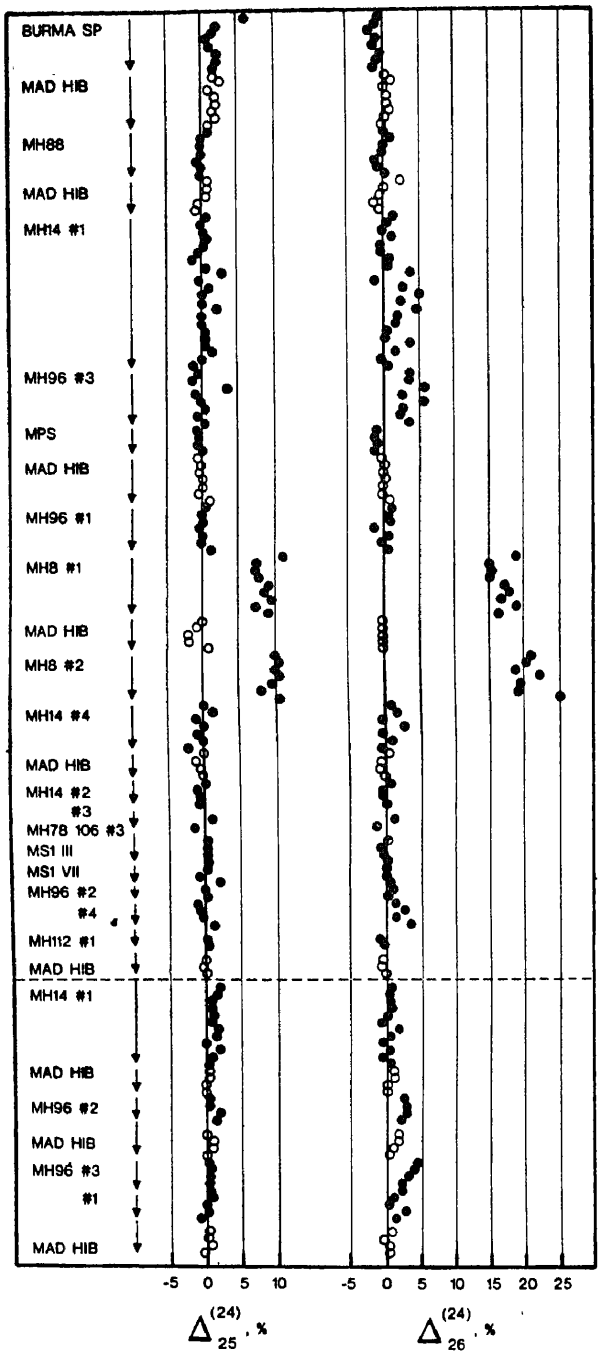

Figure 8. From Macdougall and Phinney (1979). Raw ion probe data for the Mg isotopic composition of minerals from Murchison (filled circles) and a terrestrial hibonite (open circles). The isotopic compositions are expressed in per cent deviation from normal composition. Data are recorded (top to bottom) in the sequence they were obtained; the dashed line indicates a division between two "runs" made two weeks apart. Inclusion MH8 shows large mass fractionation ; MH14 and some MH96 analyses show slight ^{26}Mg excesses. (Figure reproduced from Macdougall and Phinney, *Geophys. Res. Lett.* **6** 218 1979, copyrighted by the American Geophysical Uni n.)

topic characteristics all suggest that they are early condensates from the solar nebula. There are indications that the CM inclusions are, if anything, an earlier, more refractory condensation component than those from Allende. This is evident not only from the mineral assemblages in the CM inclusions, and the fact that their formation was completed with the condensation of the relatively high-temperature phase diopside, but also from the ultra-refractory rare earth element component which has been discovered in a Murchison inclusion (Boynton *et al* 1980). There is also suggestive evidence from the Mg isotope data that at least some of the Murchison and Allende inclusions are contemporaneous. The differences between the inclusion types in the two meteorite classes, and their similarity from one meteorite to another within the individual classes, imply different formation localities in the two cases. On the other hand, some isotopic effects—^{26}Mg excesses, fractionation effects, and most likely ^{16}O enrichments—are common to inclusions in both meteorite classes. This means that these anomalies may have been widespread, and that wherever unaltered early condensates are discovered, anomalies will be present.

Acknowledgement

We thank Jodi Carlson for technical assistance and Mary Donellan for typing the manuscript. This work was supported by NASA grant NSG 7121.

References

Allen J M, Grossman L, Davis A M and Hutcheon I D 1978 *Proc. Lunar Planet. Sci. Conf. 9th* (New York: Pergamon Press) p. 1209
Armstrong J T, Meeker G P, Huneke J C and Wasserburg G J 1980 *Meteoritics* **15** 259
Bar Matthews M, MacPherson G J, Grossman L and Tanaka T 1980 *Meteoritics* **15** 262
Black D C 1972 *Geochim. Cosmochim. Acta* **36** 347
Blander M and Fuchs L H 1975 *Geochim. Cosmochim. Acta* **39** 1605
Boynton W V 1975 *Geochim. Cosmochim. Acta* **39** 569
Boynton W V 1978 *Earth Planet. Sci. Lett.* **40** 63
Boynton W V, Frazier R M and Macdougall J D 1980 *Lunar Planet. Sci. XI* (Houston: Lunar Planet. Inst.) p. 103
Cameron A G W and Truran J W 1977 *Icarus* **30** 447
Chou C L, Baedecker P A and Wasson J T 1976 *Geochim. Cosmochim. Acta* **40** 85
Clayton D D 1977 *Icarus* **32** 255
Clayton R N and Mayeda T K 1977 *Geophys. Res. Lett.* **4** 295
Clayton R N, Grossman L and Mayeda T K 1973 *Science* **182** 485
Clayton R N, Mayeda T K and Epstein S 1978 *Proc. Lunar Planet. Sci. Conf. 9th* (New York: Pergamon Press) p. 1267
Clayton R N, Onuma N and Mayeda T K 1976 *Earth Planet. Sci. Lett.* **30** 10
Consolmagno G J and Cameron A G W 1979 *Lunar Planet. Sci.* X (Houston : Lunar Planet. Inst.) 235
Davis A M and Grossman L 1979 *Geochim. Cosmochim. Acta* **43** 1611
Davis A M, Grossman L and Allen J M 1978 *Proc. Lunar Planet. Sci. Conf. 9th* (New York : Pergamon Press) p. 1235
El Goresy A, Nagel K and Ramdohr P 1978 *Proc. Lunar Planet. Sci. Conf. 9th* (New York : Pergamon Press) p. 1279
Esat T M, Lee T, Papanastassiou D A and Wasserburg G J 1978 *Geophys. Res. Lett.* **5** 807
Falk S W, Lattimer J M and Margolis S H 1977 *Nature (London)* **270** 700
Fuchs L H, Olsen E and Jensen K J 1973 *Smithsonian Contrib. Earth Sci.* **10** 39

Grossman L 1972 *Geochim. Cosmochim. Acta* **36** 597
Grossman L 1975 *Geochim. Cosmochim. Acta* **39** 433
Grossman L 1973 *Geochim. Cosmochim. Acta* **37** 1119
Grossman L 1980 *Ann. Rev. Earth Planet. Sci.* **8** 559
Grossman L and Clark S P 1973 *Geochim. Cosmochim. Acta* **37** 635
Grossman L and Larimer J W 1974 *Rev. Geophys. Space Phys.* **12** 71
Grossman L and Ganapathy R 1976 *Geochim. Cosmochim. Acta* **40** 331
Grossman L, Bar Matthews M, Hutcheon I D, MacPherson G J, Tanaka T and Kawabe I 1980 *Meteoritics* **15** 296
Grossman L, Ganapathy R and Davis A M 1977a *Geochim. Cosmochim. Acta* **41** 1647
Grossman L, Davis A M, Olsen E and Santoliquido P M 1977b *Lunar Science* VIII (Houston: Lunar Science Inst.) p. 439.
Hutcheon I D, Bar Matthews M, Tanaka T, MacPherson G J, Grossman L and Olsen E 1980 *Meteoritics* **15** 306
Kerridge J F 1981 *12th Lunar and Planetary Science Conf.* Abstracts
Kurat G, Heinkes G and Fredriksson K 1975 *Earth Planet. Sci. Lett.* **26** 140
Lattimer J M and Grossman L 1978 *Moon and Planets* **19** 169
Lattimer J M, Schramm D N and Grossman L 1978 *Astrophys. J.* **219** 230
Lee T 1979 *Rev. Geophys. Space Phys.* **17** 1591
Lee T, Mayeda T K and Clayton R N 1980 *Geophys. Res. Lett.* **7** 493
Lee T, Papanastassiou D A and Wasserburg G J 1976 *Geophys. Res. Lett.* **3** 109
Lee T, Papanastassiou D A and Wasserburg G J 1977 *Astrophys. J. Lett.* **211** 107
Lee T, Russel W A and Wasserburg G J 1979a *Astrophys. J. Lett.* **228** 193
Lee T, Schramm D N, Wefel J and Blake B 1979b *Astrophys. J.* **232** 854
Lorin J C and Christophe Michel-Levy M 1978 *US Geol. Surv. Open File Report* 78–701, p. 297
Lugmair G W, Marti K and Scheinin N B 1978 *Lunar Planet. Sci.* **10** 672
Macdougall J D 1979 *Earth Planet. Sci. Lett.* **42** 1
Macdougall J D and Phinney D 1979 *Geophys. Res. Lett.* **6** 218
MacPherson G J and Grossman L 1979 *Meteoritics* **14** 479
Margolis S H 1979 *Astrophys. J.* **231** 236
Mason B 1975 *Acc. Chem. Res.* **8** 217
Mason B and Martin P M 1974 *Earth Planet. Sci. Lett.* **22** 141
Mason B and Martin P M 1977 *Smithsonian Contrib. Earth Sci.* **19** 84
McCulloch M T and Wasserburg G J 1978a *Astrophys. J. Lett.* **220** L15
McCulloch M T and Wasserburg G J 1978b *Geophys. Res. Lett.* **5** 599
Nagasawa H, Blanchard D P, Jacobs J W, Brannon J C, Philpotts J A and Onuma N 1977 *Geochim. Cosmochim. Acta* **41** 1587
Palme H and Wlotzka F 1976 *Earth Planet. Sci. Lett.* **33** 45
Papanastassiou D A and Wasserburg G J 1978 *Geophys. Res. Lett.* **5** 859
Papanastassiou D A and Wasserburg G J 1980 *Meteoritics* **15** 348
Tanaka T and Masuda A 1973 *Icarus* **19** 523
Tanaka T, Davis A M, Hutcheon I D, Bar Matthews M, Olsen E, MacPherson G J and Grossman L 1980 *Lunar Planet. Sci.* XI (Houston: Lunar Planet. Inst.) 1122
Wark D A 1979 *Astrophys. Space Sci.* **60** 59
Wark D A and Lovering J F 1976 *Lunar Sci.* VII (Houston: Lunar Sci. Inst.) p. 912
Wark D A and Lovering J F 1977 *Proc. Lunar Sci. Conf.* 8*th* (New York: Pergamon Press) p. 95
Wark D A and Lovering J F 1978 *Lunar Planet. Sci.* IX (Houston: Lunar Planet. Inst.) 1214
Wark D A and Lovering J F 1980 *Lunar Planet. Sci.* XI (Houston: Lunar Planet. Inst.) 1211
Wasserburg G J, Lee T and Papanastassiou D A 1977 *Geophys. Res. Lett.* **4** 299
Yeh H W and Epstein S 1978 *Lunar Planet. Sci.* IX (Houston: Lunar Planet. Inst.) 1289